

Journal of Materials Chemistry A

Accepted Manuscript



This is an *Accepted Manuscript*, which has been through the Royal Society of Chemistry peer review process and has been accepted for publication.

Accepted Manuscripts are published online shortly after acceptance, before technical editing, formatting and proof reading. Using this free service, authors can make their results available to the community, in citable form, before we publish the edited article. We will replace this *Accepted Manuscript* with the edited and formatted *Advance Article* as soon as it is available.

You can find more information about *Accepted Manuscripts* in the [Information for Authors](#).

Please note that technical editing may introduce minor changes to the text and/or graphics, which may alter content. The journal's standard [Terms & Conditions](#) and the [Ethical guidelines](#) still apply. In no event shall the Royal Society of Chemistry be held responsible for any errors or omissions in this *Accepted Manuscript* or any consequences arising from the use of any information it contains.

Supported Platinum-Zinc Oxide Core-Shell Nanoparticle Catalysts for Methanol Steam Reforming

Cite this: DOI: 10.1039/x0xx00000x

Received 00th January 2014,
Accepted 00th January 2014

DOI: 10.1039/x0xx00000x

www.rsc.org/

Lisandra Arroyo-Ramírez,^a Chen Chen,^a Matteo Cargnello,^b Christopher B. Murray,^{b,c} Paolo Fornasiero^d and Raymond J. Gorte^a

Platinum-zinc oxide (Pt@ZnO) and palladium-zinc oxide (Pd@ZnO) core-shell nanoparticles were synthesized in solution using a method based on self-assembly and deposited onto a functionalized alumina (Si-Al₂O₃) support. TEM investigations of the samples confirm the formation of core-shell structures of approximately 6 nm of diameter following calcination to remove the ligands. In-situ TEM and coulometric titration experiments suggest that Pt-Zn alloys are formed upon reduction and that these are highly tunable in size. While methanol-steam reforming (MSR) measurements on conventional Pt/Al₂O₃ and Pd/Al₂O₃ catalysts show poor CO₂ selectivities, a Pt(1-wt.%)@ZnO(9-wt.)/Si-Al₂O₃ system showed comparable activity and selectivity for CO₂ as a conventional Pt/ZnO catalyst, providing further indication that Pt@ZnO forms a Pt-Zn alloy upon reduction due to the intimate contact between the two materials. The Pd@ZnO/Si-Al₂O₃ exhibited lower CO₂ selectivities than Pt@ZnO/Si-Al₂O₃.

Introduction

Methanol is a potentially convenient vehicle for storing hydrogen that could then be used in fuel-cell vehicles. It is relatively easy to convert methanol to hydrogen by the methanol steam reforming (MSR) reaction due to its high H/C ratio and absence of C-C bonds, allowing the reaction to take place at relatively low temperatures.¹ An important goal with MSR catalysts is to obtain high selectivity to CO₂, rather than CO, so as to avoid the need for a water-gas-shift catalyst.² To achieve this goal, various metals of group VIII have been studied on different supports as potential catalysts for MSR.⁴⁻⁶

ZnO exhibits interesting properties as a support and as a promoter for Pt and Pd catalysts.²⁻⁴ The relatively facile reduction of ZnO and subsequent formation of PtZn and PdZn alloys lead to strikingly different catalytic activities compared to the bare metals. For example, PtZn alloys formed from Pt/ZnO catalysts were found to be selective for hydrogenation of α,β -unsaturated aldehydes to the corresponding saturated alcohols.⁷ It has been shown that the addition of Zn to Pt(111) surface changes the reactivity of platinum, the catalysts becoming more selective for deoxygenation of aldehydes and methanol steam reforming (MSR) reaction due to the formation of PtZn alloy.^{8,9} Similarly, Zn-promoted, carbon-supported Pt and Pd catalysts are selective for methanol steam reforming, with CO₂ being the

primary product, rather than CO.^{10,11} Also, Pd/ZnO has shown high CO₂ selectivity in the MSR reaction due to the formation of an alloy phase.¹² Other studies demonstrated that the particle size of the PdZn alloy can affect the selectivity for the MSR.^{13,14,22}

The methods used for the preparation of the catalysts affect the activity and selectivity for MSR and this has been reviewed.² Structural and compositional heterogeneity are important considerations for any supported-metal catalyst but they are especially important with alloys. For example, most Pt/ZnO catalysts formed by impregnation of Pt salts onto a ZnO support would have Pt particles with wide size distributions.¹¹ Pt-Zn alloys form upon reduction, but the Pt:Zn ratio depends on the reduction conditions and the initial Pt particle size. If Zn salts are added to an existing supported-metal catalyst, only a fraction of the Zn will end up interacting with the metal component, and a significant excess of Zn has to be added in order to ensure contact between Zn and Pt components.¹¹ These issues bring the challenge of finding preparation methods that allow fine tuning of the composition and morphology of the catalysts.

Recent work from our laboratories has provided a method for achieving homogeneous materials with uniform particle sizes and compositions, with good contact between precious metals and oxide phases.¹⁵ The method involves preparing metal nanoparticles with oxide shells in solution, then adsorbing these core-shell particles onto an inert support. Uniform metal

particles are produced by reduction of a metal salt in the presence of a bifunctional ligand, 11-mercaptoundecanoic acid (MUA), in an organic solvent.^{16,17} Uniform oxide shells are then formed around the metal nanoparticles by reaction of a metal alkoxide with the carboxylic acid end group of the MUA ligand. Following a controlled hydrolysis of the remaining alkoxide groups in the presence of an organic acid, well defined, core-shell particles are produced and remain stable and dispersed in the organic solvent. Finally, the dispersed core-shell structures can be deposited onto engineered oxide supports in monolayer form, then calcined to remove the remaining ligands. Using these methods, Pd and Pt nanoparticles have been prepared with CeO₂, ZrO₂, and TiO₂ shells.¹⁷

Here, we demonstrate that Pt@ZnO and Pd@ZnO core-shell catalysts of uniform size and composition can be prepared by methods similar to those used previously.¹⁶ The core-shell particles can again be adsorbed from solution onto functionalized-alumina supports. In-situ TEM and coulometric titration experiments suggest the formation of alloyed particles of controlled size. The catalytic activity and selectivity of the systems for MSR are also shown to be in agreement with the formation of the alloys. This work provides a general method to prepare alloyed particles of tunable size and composition starting with well defined core-shell building blocks.

Experimental Section

Materials

Potassium tetrachloroplatinate(II) (K₂PtCl₄, 98%), potassium tetrachloropalladate(II) (K₂PdCl₄, 98%), diethylzinc (Zn 52.0 wt. %), 11-mercaptoundecanoic acid (MUA, 95%), anhydrous 1-butanol (99.8%), and triethoxy(octyl)silane (TEOOS, ≥97.5 %) were purchased from Sigma–Aldrich. Dodecylamine (CH₃(CH₂)₁₁NH₂, 98%), lithium triethylborohydride (1.0 M LiBEt₃H in THF) and dodecanoic acid (CH₃(CH₂)₁₀COOH, 99%) were purchased from Acros Organics. Anhydrous magnesium sulfate was purchased from Fisher-Scientific. Sodium borohydride (NaBH₄, 98%), tetraammineplatinum(II) nitrate (Pt(NH₃)₄(NO₃)₂, 99.99%), tetraamminepalladium(II) nitrate solution ((NH₃)₄Pd(NO₃)₂, 99.9%), tetraoctylammonium bromide (TOABr, 98%+) and zinc oxide powder (ZnO, 99.9%, 42 m² g⁻¹) were purchased from Alfa Aesar. Al₂O₃ powder (Puralox TH100/150) was purchased from Sasol and calcined to 1173 K for 24 h prior to use (surface area 90 m² g⁻¹). All of the solvents were HPLC grade from Fisher-Scientific.

Synthesis of the catalysts

MUA-protected Pt nanoparticles (Pt-MUA in tetrahydrofuran, THF) were prepared following previously reported procedures.¹⁷ Briefly, K₂PtCl₄ was dissolved in deionized water and transferred to CH₂Cl₂ using TOABr as phase-transfer agent. The aqueous phase was discarded and the organic phase was dried with anhydrous magnesium sulfate. Dodecylamine was added and the reaction vessel was purged with N₂ until after the Pt reduction step. The reducing agent (LiBEt₃H) was added rapidly, with vigorous stirring, causing the solution to change from orange to black. The solution was then stirred for an additional 5 min. Next, the reaction mixture was washed with water and the solvent removed by evacuation. Ethanol was added to the black solid, which was then centrifuged three times to remove the excess of dodecylamine and TOABr. After dissolving the Pt-dodecylamine nanoparticles in a CH₂Cl₂/THF solution, MUA

was added and the solution stirred overnight. After again removing the solvent by evacuation, the solid was washed with CH₂Cl₂ and centrifuged three times to remove excess dodecylamine. Finally, the black solid (Pt-MUA) was redissolved in THF. The Pd-MUA nanoparticles were prepared following previously reported procedures.¹⁶

The synthesis of zinc butoxide (Zn(OBu)₂) was carried out in a nitrogen-filled glove box (<0.1 ppm of water and O₂) following previously reported procedures, with only slight modifications.¹⁸ Diethyl zinc ((C₂H₅)₂Zn, 1 mmol) was added dropwise to anhydrous 1-butanol (C₄H₉OH, 5 mL) with vigorous stirring. (Caution: Flammable gas is generated in this process and the reaction is exothermic.) The zinc butoxide solution produced in this reaction is stable under air exposure for a limited period of time and was therefore taken out of the glove box and used immediately without further purification. The functionalized, hydrophobic alumina (Si-Al₂O₃) was prepared by allowing pristine Al₂O₃ (10 g) to react with TEOOS (5.8 mL) in toluene (30 mL).¹⁵ The solution was refluxed for 6 hours, filtered, and washed several times with toluene to remove unreacted TEOOS. The powder was dried in air overnight at 383 K.

Preparation of the catalyst Pt(1-wt%)/ZnO(9-wt%)/Si-Al₂O₃ was similar to published procedures.^{16,17} An appropriate volume of Pt-MUA solution was added dropwise to an appropriate amount of Zn(OBu)₂ solution under constant stirring to achieve the final desired loadings. Dodecanoic acid (1 mol per Zn), dissolved in THF, was added to the dispersed particles, after which the hydrolysis was carried out by slowly adding a solution containing 0.5 mL H₂O in 10 mL of THF over a period of two hours. Next, the Si-Al₂O₃ was slowly added to the Pt@ZnO solution and the slurry was stirred overnight. During this period, the Pt@ZnO nanostructures were adsorbed onto the Si-Al₂O₃ support, as evidenced by the solution turning from black to translucent white (The translucent white appearance is likely due to a small amount of Al₂O₃ or ZnO remaining suspended in solution.). Next, the solvent was removed by rotary evaporation. Finally, the Pt@ZnO/Si-Al₂O₃ sample was calcined in flowing air at 773 K for 6 h, using a heating ramp of 3 K min⁻¹. The Pd@ZnO/Si-Al₂O₃ sample was prepared following the same procedure described above but using the Pd-MUA solution.

Conventional Pt/ZnO, Pt/Al₂O₃, Pd/ZnO, Pd/Al₂O₃ catalysts with 1-wt% metal were also prepared for comparison purposes by wet impregnation of ZnO or Al₂O₃ with aqueous solutions of Pt(NH₃)₄(NO₃)₂ and (NH₃)₄Pd(NO₃)₂, respectively. The dried powders were calcined in air at 773 K for 6 h using a heating ramp of 3 K min⁻¹.

Characterization

Transmission electron microscopy (TEM) images were obtained using a JEOL 2100 microscope, with an accelerating voltage of 200 kV. CO chemisorption measurements were performed using a home-built adsorption apparatus. To prepare the samples for chemisorption measurements, the calcined sample was first exposed to 200 Torr O₂ at 673 K for 2 min and then evacuated. This pre-treatment was repeated three times. Next, the sample was exposed to 200 Torr of H₂ at either 423 or 673 K for 5 min, followed by evacuation. This reduction step was again repeated three times. CO chemisorption was performed at room temperature by adding small pulses of CO to the sample until a pressure rise in the sample cell was detected.

A detailed description of the coulometric titration apparatus is given elsewhere.¹⁹ Briefly, 1 g of Pt@ZnO/Si-Al₂O₃ sample that was calcined at 1073 K was put in an aluminium crucible and inserted inside a yttria-stabilized zirconia (YSZ) tube with

Ag electrodes that were painted on the inside and outside. After the apparatus was heated to 873 K, a mixture of 5% O₂, 11% H₂O and 84% Ar was introduced through the YSZ tube for 1 h, and the two ends of the tube were then sealed. The measurement of the redox isotherms was performed by electrochemically pumping controlled amounts of oxygen into the YSZ tube via the application of a voltage across the electrodes using a potentiostat (Gamry Instruments). The amount of oxygen transferred was quantified by integrating the current, and the system was allowed to reach equilibrium (when open-circuit voltage changes are less than 3 mV/day). The equilibrium P(O₂) was determined from the open-circuit potential using the Nernst equation. After obtaining the reduction isotherm, oxygen was added in controlled volumes to get the oxidation isotherm to confirm reversibility.

Rate and selectivity for methanol steam reforming (MSR) reaction were measured in a ¼ inch, quartz, tubular reactor at atmospheric pressure. 0.10 g of sample were loaded into the reactor and held in place with glass wool. Prior to MSR activity tests, the catalysts were reduced in flowing 5% H₂-He mixtures at 523 K for 30 min. After cooling to 453 K in flowing He, methanol/water mixture with partial pressure of 45 torr MeOH and 45 torr H₂O were introduced into the reactor with He as a carrier gas. The total volumetric flow rate in the reactor was kept to 110 mL min⁻¹. Products were analyzed using an online gas chromatograph (SRI8610C) equipped with a HayeSep Q column and a TCD detector. The catalytic activity and CO₂ selectivity were calculated on a carbon basis. The selectivity to CO₂ was defined as $S = (\text{moles CO}_2) / ((\text{moles CO}_2) + (\text{moles CO}))$.

Results and Discussions

The supported Pt@ZnO and Pd@ZnO core-shell nanostructures were prepared in solution by self-assembly methods discussed above. Temperature-programmed-oxidation (TPO) (Fig. S1, Supporting Information) experiments on the uncalcined Pt@ZnO/Si-Al₂O₃ sample show that the decomposition of the ligands begins at approximately 400 K and that there is a peak in the oxygen consumption centered at 525 K (Fig. S1). Slightly higher temperatures (575 K) are required to remove the ligands in Pd@ZnO/Si-Al₂O₃ compared to Pt@ZnO/Si-Al₂O₃. A previous study of Pd@CeO₂/Si-Al₂O₃ shows the O₂-consumption peak at 480 K.²⁰ The temperature in which the ligands are removed from the samples depends on the metal and the oxide used; but, for all the samples, the ligands were removed by 650 K. For all studies in this paper, the samples were calcined at 773 K to form the core-shell nanostructures.

Transmission electron microscopy (TEM) investigations were performed to understand nanoparticle morphology and particle size. Figure 1 shows representative TEM images of the Pt@ZnO/Si-Al₂O₃ calcined at 773 K in air. The low resolution TEM images (Fig. 1A-B) show the core-shell particles distributed throughout the Si-Al₂O₃ support and the high magnification TEM images (Fig. 1C-F) show the morphology of the core-shell nanostructures. The images show dark Pt cores surrounded by a crystalline ZnO shell supported onto the alumina grains. The Pt cores are about 2 nm in diameter, the same as the starting Pt-MUA nanoparticles,¹⁷ demonstrating that there was no agglomeration of the metal particles after calcination at 773 K. The entire core-shell nanostructures have a diameter of approximately 6 nm, from which a 2 nm-thick ZnO shell is

measured. This thickness is similar to what observed in the case of titania, zirconia and ceria¹² and demonstrates the successful implementation of the procedure to the Pt-ZnO combination. The oxide shells in this synthesis procedure are limited to 2 nm by the number of carboxyl end groups present in the MUA ligands surrounding the dispersed metal nanoparticles.

It was possible to observe the formation of Pt-Zn alloy in the TEM due to the reducing power of the electron beam. Figure 2 reports a series of images taken at 20-s intervals where the initial Pt-ZnO core-shell particle dispersed onto the alumina support transforms into a slightly larger Pt-Zn core surrounded by a thinner ZnO shell. During alloy formation, the core Pt particle lose their crystalline morphology (Fig. 2A) to transform into the disordered alloy (Fig. 2D). Figure S2 shows the representative TEM images for the Pd@ZnO/Si-Al₂O₃ core-shell sample. Despite the lower contrast between Pd and the oxide, the ~2 nm metal cores are discernible also in this case and the metal particles are again surrounded by a ~2 nm oxide shell.

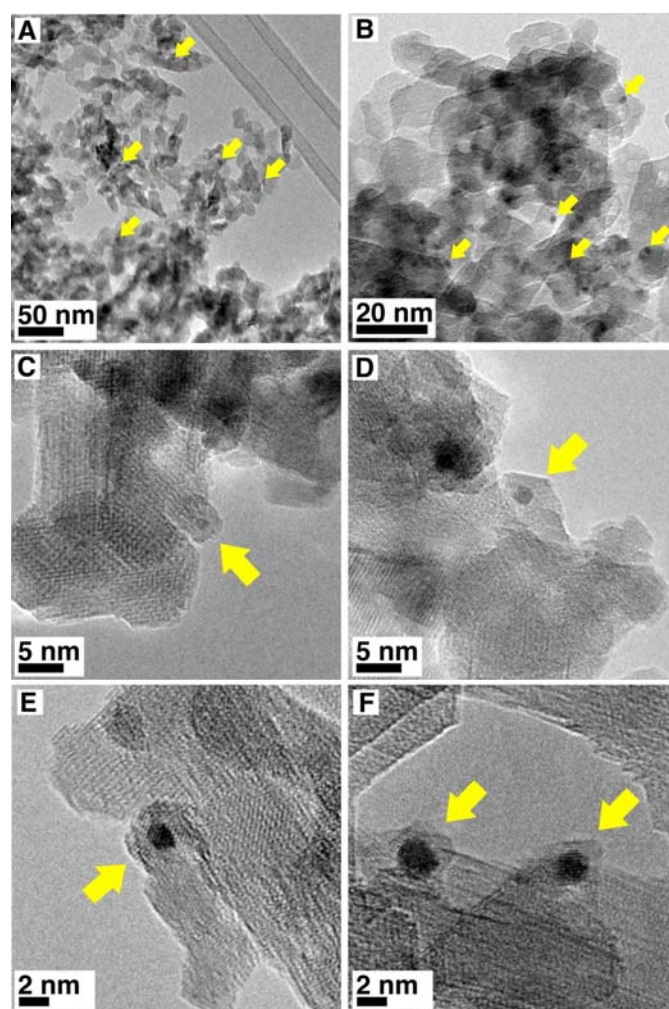


Fig. 1 Representative low (A, B) and high (C-F) resolution transmission electron microscopy (TEM) images of Pt@ZnO/Si-Al₂O₃ sample calcined at 773 K in air. Yellow arrows point to core-shell structures where the higher contrast is attributed to Pt cores surrounded by a lighter, ZnO shell.

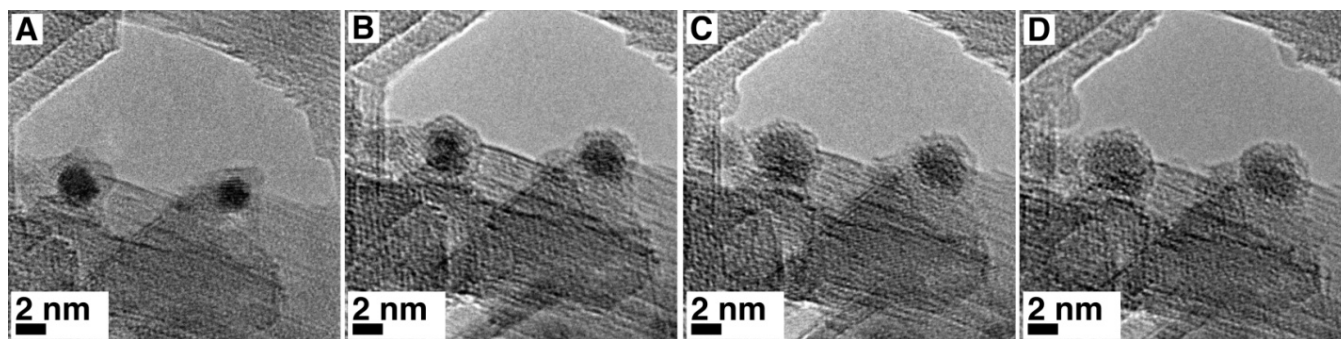


Fig. 2 TEM images taken at 20 s interval (from A to D) of two Pt@ZnO core-shell structures (A) that progressively transform into Pt-Zn alloyed particles under the electron beam irradiation. The images were taken at 200 kV.

X-ray diffraction (XRD) of the Pt/ZnO sample showed very low intensity and broad peaks near 2θ angles of 39.6° and 46.1° which can be attributed to Pt (111) and Pt (200) family of planes, respectively (Fig. S3D). In the Pt/ZnO sample, a crystallite size of 45 nm was calculated using the Scherrer equation. Pt-Zn alloy was formed as evidenced by the lattice parameter shift in the Pt/ZnO (0.3942 nm) compared to that of pure platinum (0.3923 nm).²¹ The XRD pattern of the sample Pt@ZnO/Si-Al₂O₃ was dominated by the alumina peaks and only a broad, low intensity peak at $\sim 56^\circ$ that can be attributed to ZnO was discernible (Fig. S3E). Similar results were obtained for the Pd and Pd@ZnO/Si-Al₂O₃ catalysts (Fig. S4). The small crystallite size and the low loadings effectively prevent observation of the PtZn and PdZn XRD peaks.

Table 1 Metal apparent dispersions (%) based on CO uptake at room temperature for the calcined samples after different pre-treatment conditions.

Sample	1 st Reduction at 423 K	2 nd Reduction at 673 K	3 rd Reduction at 423 K
Pt@ZnO/Si-Al ₂ O ₃	4	0	2
Pt/Al ₂ O ₃	34	41	32
Pt/ZnO	3	0	2
Pd@ZnO/Si-Al ₂ O ₃	3	4	2
Pd/ZnO	1	1	1
Pd/Al ₂ O ₃	22	18	19

CO chemisorption results are reported in Table 1. In contrast to what is observed for the Pt/Al₂O₃ sample, which shows appreciable CO uptakes, both Pt/ZnO and Pt@ZnO/Si-Al₂O₃ samples show very low CO uptakes corresponding to Pt dispersion values well below 5%. For conventional catalysts, this would imply particle sizes of the order of 10 nm. This result is clearly in contrast with TEM investigations (Fig. 1), which showed the presence of small (2 nm), well dispersed Pt particles

in the core-shell catalyst. The low adsorption uptake is likely due to formation of the Pt-Zn alloy, which has much reduced adsorption compared to the pure Pt particles present in the Pt/Al₂O₃ system. It is noteworthy that reduction at higher temperatures decreases the CO uptake to almost zero for the ZnO-containing samples. The low CO chemisorption uptake for the core-shell sample can also be explained by the ZnO shell which coats part of the Pt surface as has been observed for other core-shell systems.¹⁷ For Pd@ZnO/Si-Al₂O₃, reduction at 673 K slightly increases the dispersion. Oxidizing the samples restores the initial chemisorption values, providing evidence that alloy formation is primarily responsible for the reduced adsorption capacity.

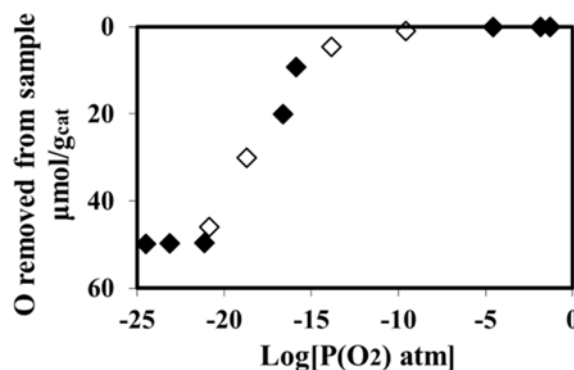


Fig. 3 Redox isotherms for Pt@ZnO/Si-Al₂O₃ at 873 K. Closed symbols were obtained starting from the oxidized state. Open symbols were measured while re-oxidizing the sample.

Coulometric titration experiments were also performed on the supported Pt@ZnO core-shell catalyst. Coulometric titration is an equilibrium, electrochemical technique for measuring oxidation state as a function of $P(O_2)$. Figure 3 shows the redox isotherm for the Pt@ZnO/Si-Al₂O₃ sample at 873 K. Only a single reduction step was observed in the $P(O_2)$ range of 10^{-15} – 10^{-20} atm, which is close to the calculated $P(O_2)$ for ZnO-Zn equilibrium, 2.3×10^{-16} atm. The amount of oxygen that could be removed from the sample is about $50 \mu\text{mol g}^{-1}$, corresponding to

an O/Pt ratio of 1, further indicating the formation of a PtZn alloy. Interestingly, most of the ZnO in the core-shell catalyst is not being reduced in this experiment, possibly because of interactions with the alumina support. The results also imply that PtZn alloy formation does not significantly affect the Zn-ZnO equilibrium. The temperature programmed reduction (TPR) profile for the Pt@ZnO/Si-Al₂O₃ shows two peaks, the first of which corresponds to the reduction of ZnO in contact with Pt. Approximately 55 μmol g⁻¹ of oxygen is removed in this low-temperature feature, a result that correlates well with the coulometric titration results for the formation of the PtZn alloy.

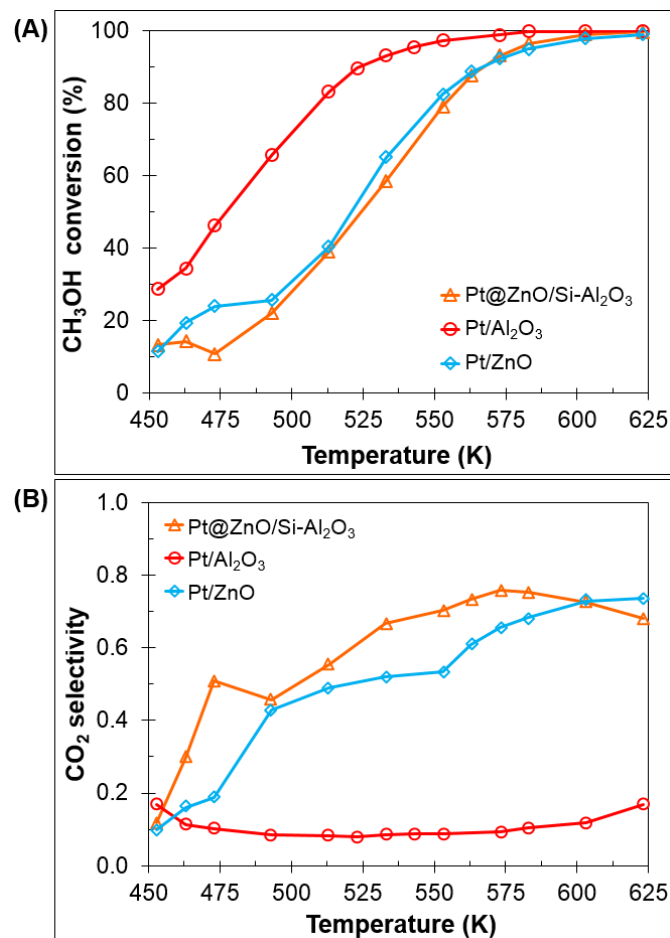


Fig. 4 (A) Methanol steam reforming (MSR) catalytic activity and (B) CO₂ selectivity over the Pt@ZnO/Si-Al₂O₃ core-shell (triangle symbol), and conventional Pt/Al₂O₃ (circle symbol) and Pt/ZnO (diamond symbol) calcined at 773 K. The catalysts were pretreated in a reducing (5% H₂/He) atmosphere at 523 K for 30 minutes. All catalysts with 1 wt% of Pt.

The core-shell structures were tested as catalysts for methanol steam reforming ($\text{CH}_3\text{OH} + \text{H}_2\text{O} \rightarrow \text{CO}_2 + 3\text{H}_2$), with light-off curves for Pt@ZnO/Si-Al₂O₃ and conventional Pt/Al₂O₃ and Pt/ZnO catalysts shown in Fig. 4A. Before the reaction, each of the materials was exposed to flowing H₂ at 523 K for 30 min. Reaction occurred at lower temperatures on Pt/Al₂O₃, with nearly complete conversion of the CH₃OH by 550 K. The reaction started at higher temperatures on Pt@ZnO/Si-Al₂O₃ and Pt/ZnO, with complete conversion requiring 600 K. However, the selectivities to CO₂ with Pt@ZnO/Si-Al₂O₃ and Pt/ZnO were much higher than that with Pt/Al₂O₃, as shown in Fig. 4B. At 573 K, the selectivity to CO₂ was 66% on Pt/ZnO,

76% on Pt@ZnO/Si-Al₂O₃ and less than 10% on Pt/Al₂O₃. The formation of alloy phases increases the CO₂ selectivity compared to metallic phase.

Similar trends were observed with the Pd-based catalysts. For a given temperature, the conversions were highest with Pd/Al₂O₃, as shown in Figure 5A. However, as shown in Figure 5B, the selectivities for CO₂ were much higher on the Pd/ZnO and Pd@ZnO/Si-Al₂O₃ catalysts. The conventional Pd/ZnO exhibited somewhat higher selectivities than did the Pd@ZnO core-shell catalyst, possibly due to particle size effects. Conant et al. observed that smaller crystallites of Pd-Zn alloys were less selective than larger particles.²² However, in all cases, the Pd-Zn alloy catalysts were more selective for CO₂ than their pure Pd analogues. This agrees with previous observations that the selectivity of ZnO-supported catalysts in MSR depends on the reduction temperature.^{12,23-25}

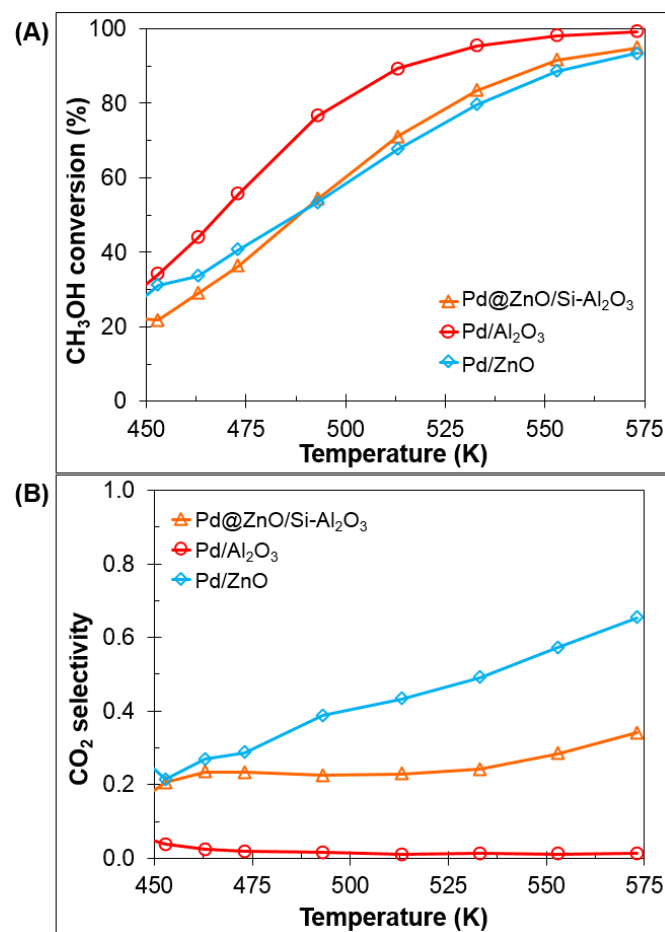


Fig. 5 (A) Methanol steam reforming (MSR) catalytic activity and (B) CO₂ selectivity over the Pd@ZnO/Si-Al₂O₃ core-shell (triangle symbol), and conventional Pd/Al₂O₃ (circle symbol) and Pd/ZnO (diamond symbol) calcined at 773 K. The catalysts were pretreated in a reducing (5% H₂/He) atmosphere at 523 K for 30 minutes. All catalysts with 1 wt% of Pd.

What we have demonstrated in this paper is that the procedures developed in previous work for making hierarchical core-shell catalysts can be extended to include ZnO shells. An advantage of these materials is that the core-shell particles are highly uniform, both in their metal diameters and shell thicknesses. These core-shell particles can also be attached to any functionalized surface.²⁶ Therefore, the self-assembly

method can be useful for the synthesis of heterogeneous catalysis with highly tailored and tunable properties.

Conclusions

We successfully demonstrated the preparation of Pt@ZnO and Pd@ZnO core-shell nanostructures, well dispersed on a functionalized alumina support. TEM images proved the formation of Pt@ZnO and Pd@ZnO core-shell nanostructures of 6 nm in diameter composed of a metal core of ~2 nm surrounded by an homogeneous ZnO shell of ~2 nm. Coulometric titration experiments, TPR, and methanol steam reforming (MSR) results strongly suggest that the metal core-oxide shell structures can form alloys upon mild reduction. The MSR results show that Pt/Al₂O₃ and Pd/Al₂O₃ catalysts have catalytic activity with poor CO₂ selectivity, while the alloy catalysts (Pt@ZnO/Si-Al₂O₃ and Pd@ZnO/Si-Al₂O₃) have higher CO₂ selectivity. These findings present a controlled method for preparing alloys for heterogeneous catalysis.

Acknowledgements

LAR acknowledges support from the University of Pennsylvania Provost Academic Diversity Fellowship. CC and RJG thank the U.S. Department of Energy (Project DE-SC0009440), Department of Energy, Office of Basic Energy Sciences, Chemical Sciences, Geosciences and Biosciences Division (Grant No. DE-FG02-13ER16380). MC and CBM acknowledge the National Science Foundation - Nano/Bio Interface Center at the University of Pennsylvania (Grant DMR08-32802) and the Richard Perry University Professorship.

Notes and References

^a Department of Chemical and Biomolecular Engineering, University of Pennsylvania, 311A Towne Building, 220 South 33rd Street, Philadelphia, PA 19104, USA.

^b Department of Chemistry, University of Pennsylvania, 231 South 34th Street, Philadelphia, PA 19104, USA.

^c Department of Materials Science and Engineering, 3231 Walnut Street, Philadelphia, PA 19104, USA.

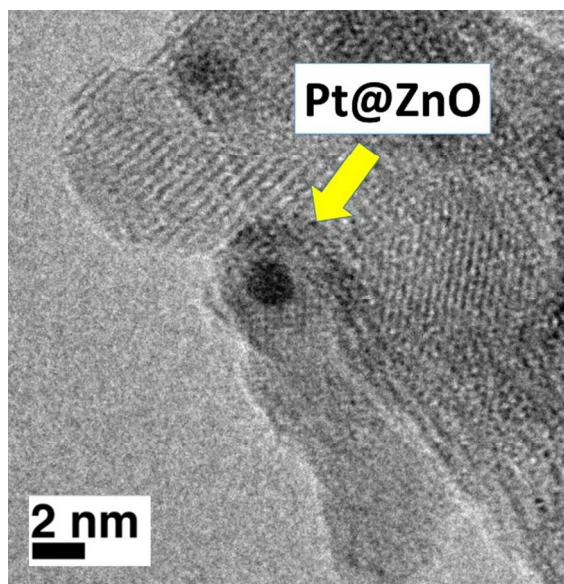
^d Department of Chemical and Pharmaceutical Sciences, ICCOM-CNR, Consortium INSTM, University of Trieste, via L. Giorgieri 1, 34127 Trieste, Italy.

† Electronic Supplementary Information (ESI) available: Experimental section, TPO curves, TEM image of Pd@ZnO/Si-Al₂O₃, XRD patterns, TPR profile and table of MSR activity and selectivity. See DOI: 10.1039/b000000x/

- 1 J. Agrell, H. Birgersson, M. Boutonnet, I. Melián-Cabreara, R. M. Navarro, J. L. G. Fierro, *J. Catal.* 2003, **219**, 389
- 2 S. Sá, H. Silva, L. Brandão, J.M. Sousa, A. Mendes *Appl. Catal. B*, 2010, **99**, 43.
- 3 W. Tong, A. West, K. Cheung, K.-M. Yu, S.C.E. Tsang, *ACS Catal.*, 2013, **3**, 1231.
- 4 N. Iwasa, T. Mayanagi, N. Ogawa, K. Sakata, N. Takezawa, *Catal. Lett.*, 1998, **54**, 119.
- 5 M. Armbrüster, M. Behrens, K. Föttinger, M. Friedrich, É. Gaudry, S.K. Matam, and H.R. Sharma, *Cat. Rev. - Sci. Eng.* 2013, **55**, 289.

- 6 R. L. Barbosa, V. Papaefthimiou, Y. T. Law, D. Teschner, M. Hävecker, A. Knop-Gericke, R. Zapf, G. Kolb, R. Schlögl, S. Zafeiratos, *J. Phys. Chem. C* 2013, **117**, 6143.
- 7 F. Ammaria, J. Lamotte, R. Touroude, *J. Catal.*, 2004, **221**, 32.
- 8 McManus J.R., Martono E., Vohs, J.M. *ACS Catal.*, 2013, **3**, 1739.
- 9 E. Martono, J.M. Vohs, *J. Phys. Chem. C*, 2013, **117**, 6692.
- 10 Y. Suwa, S.-I. Ito, S. Kameoka, K. Tomishige, K. Kunimori, *Appl. Catal. A*, 2004, **267**, 9.
- 11 S.-I. Ito, Y. Suwa, S. Kondo, S. Kameoka, K. Tomishige, K. Kunimori, *Catal. Commun.*, 2003, **4**, 499.
- 12 N. Iwasa, N. Takezawa, *Top. Catal.*, 2003, **22**, 215.
- 13 A. Karim, T. Conant, A. Datye, *J. Catal.* 2006, **243**, 420.
- 14 R. A. Dagle, Y.-H. Chin, Y. Wang, *Top. Catal.* 2007, **46**, 358.
- 15 M. Cargnello, J.J. Delgado Jaén, J.C. Hernández Garrido, K. Bakhmutsky, T. Montini, J.J. Calvino Gámez, R.J. Gorte, P. Fornasiero, *Science*, 2012, **337**, 713.
- 16 M. Cargnello, N.L. Wieder, T. Montini, R.J. Gorte, P. Fornasiero, *J. Am. Chem. Soc.*, 2010, **132**, 1402.
- 17 K. Bakhmutsky, N.L. Wieder, M. Cargnello, B. Galloway, P. Fornasiero, R.J. Gorte, *ChemSusChem*, 2012, **5**, 140.
- 18 A. Cote, A.B. Charette, *J. Am. Chem. Soc.*, 2008, **130**, 2771.
- 19 I. Baldychev, R.J. Gorte, J.M. Vohs, *J. Catal.* 2010, **269**, 397
- 20 C. Chen, J. Cao, M. Cargnello, P. Fornasiero, R.J. Gorte, *J. Catal.*, 2013, **306**, 109.
- 21 Powder Diffraction File, JCPDS card no. 04-0802.
- 22 Conant T., A.M. Karima, V. Lebarbier, Y. Wang, F. Girgsdies, R. Schlögl, A. Datye, *J. Catal.*, 2008, **257**, 64.
- 23 L. Li, B. Zhang, E. Kunkes, K. Föttinger, M. Armbruster, D.S. Su, W. Wei, R. Schlögl, M. Behrens, *ChemCatChem*, 2012, **4**, 1764.
- 24 A. Haghofers, K. Föttinger, F. Girgsdies, D. Teschner, A. Knop-Gericke, R. Schlögl, G. Rupprechter, *J. Catal.*, 2012, **286**, 13.
- 25 H. Lorenz, S. Penner, W. Jochum, C. Rameshan, B. Klötzer, *Appl. Catal. A*, 2009, **358**, 203.
- 26 L. Adjianto, D. A. Bennett, C. Chen, A. S. Yu, M. Cargnello, P. Fornasiero, R. J. Gorte, J. M. Vohs, *Nanoletters*, 2013, **13**, 2252.

Table of contents



Pt@ZnO and Pd@ZnO core-shell structures have been synthesized and shown to form alloy catalysts with good CO₂ selectivity for MSR.